Hunt, J.M., J.K. Whelan, L.B. Eglinton, and L.M. Cathles III, 1998, Relation of shale porosities, gas generation, and compaction to deep overpressures in the U. S. Gulf Coast, *in* Law, B.E., G.F. Ulmishek, and V.I. Slavin eds., Abnormal pressures in hydrocarbon environments: AAPG Memoir 70, p. 87–104.

Chapter 5

Relation of Shale Porosities, Gas Generation, and Compaction to Deep Overpressures in the U.S. Gulf Coast

John M. Hunt
Jean K. Whelan
Lorraine Buxton Eglinton
Woods Hole Oceanographic Institution
Woods Hole, Massachusetts, U.S.A.

Lawrence M. Cathles III
Department of Geological Sciences
Cornell University
Ithaca, New York, U.S.A.

Abstract

Direct measurements of porosities from Tertiary and Cretaceous shales in the Texas-Louisiana Gulf Coast show that in many areas shale porosity is either constant or increasing at the depths where high overpressures occur and where hydrocarbons are being generated. In the absence of a decrease in porosity with sediment load (depth), gas generation becomes the principal cause of overpressures and hydrocarbon expulsion.

Gulf Coast shale porosities decrease exponentially in normally compacting shales only down to porosities of about 30%, after which the decrease is linear until a constant porosity is reached. These linear trends are believed to be related to the high quartz content (74%) of the clay-size fraction (<4 microns).

The depths at which shales reach relatively constant porosity values appear to depend on the internal surface areas of the shales. Shales containing minerals with small, internal surface areas, such as fine-grained quartz and carbonates, stop compacting at porosities around 3%, whereas shales containing minerals with large surface areas, such as smectite and illite, stop compacting around 10%. This interval of no compaction usually is reached at depths around 3 to 4 kilometers (temperatures of 85° to 110°C) prior to the development of deep high overpressures and the generation of large quantities of hydrocarbons in the Gulf Coast. Model studies indicate that gas generation is the dominant process creating these deep overpressures.

The porosity-depth profiles that show a linear decrease with depth followed by a constant porosity do not conform to the hypothesized exponential profiles used in many modeling programs today. This means that more direct shale porosity measurements are needed to confirm the type of profiles that actually exist and should be used in any basin modeling program.

INTRODUCTION

Compaction is defined as the loss of porosity due to stress. Shales showing no loss in porosity through thousands of feet of burial indicate no compaction. The objectives of this paper are to show how direct porosity measurements made on both cuttings and cores from many wells in the U.S. Gulf Coast indicate the following three points:

1. Under hydrostatic conditions shale porosities below about 30% tend to decrease linearly (not exponentially) with depth to a point below which there is no further decrease.
2. The cessation of compaction does not appear to be related to overpressuring. This phenomenon occurs with normally pressured shales. The two-stage, linear compaction is thus a "normal" compaction trend.

3. At depths where compaction no longer occurs, gas generation seems to be the major cause of overpressures and the probable cause of hydrocarbon expulsion from source rocks.

Two kinds of porosity-depth curves for shales have been published over the past several decades. Composites of porosity-depth data from several wells over a large area generally show a scatter of data points through which an exponential porosity curve can be drawn. Such curves indicate a rapid decrease in porosity near the surface and a slower decrease with increasing depth. Several examples and their variability are discussed by Rieke and Chilingarian (1974, p. 42), Dickey (1976) and Hunt (1979, p. 202). The second type of curve, which is best recognized from analyses of single wells rather than composites, shows that after an initial exponential decrease to 30–35% porosity, the subsequent porosity decrease follows two straight-line segments in angular end-to-end contact with each other. The second line frequently has no slope, thus indicating no compaction.

Hedberg (1936) was the first to observe this latter phenomenon in undisturbed Tertiary shales of the Eastern Venezuelan Basin (Figure 1). Most of his data were from a single well supplemented with a few shallow and deep data points from two other wells in the same area.

Hedberg described four stages in the compaction of shales, the first three due to mechanical compaction and the last to chemical compaction. These stages were described as mechanical rearrangement for porosity decreasing from 90 to 75%, dewatering from 75 to 35%, mechanical deformation from 35 to 10%, and recrystallization, i.e., chemical compaction for porosity decreases to below 10%. Hedberg observed that, "reduction of pore space below 10% takes place very slowly and only with large increments of pressure. Chemical readjustment becomes the dominant factor in the fourth stage of compaction." Hedberg's division of mechanical compaction and chemical compaction or diagenesis for the Venezuelan shales at around 10% porosity becomes important in our later discussion of a two stage model for the decrease in the porosity of shales with depth.

In 1959, Storer published dry bulk density-depth curves for several wells in the Po Basin of Italy. They showed some of the same linear changes reported by Hedberg. Linear shale compaction trends also have been reported by Korvin (1984) and Wells (1990).

Many of the Tertiary shales from the Gulf Coast discussed in this paper show little change in porosity at depths >3 km whereas sandstones show a wide variation. Loucks et al. (1984) analyzed sandstone porosities in 7,564 cores from the Lower Tertiary of the Texas Gulf Coast. They found that porosities ranged from 3 to 30% at various depths between 9,000 and 15,000 feet (2,440 and 4,570 m). Over half of the total porosity below 10,000 ft (3,050 m) was secondary due to chemical diagenesis. They observed that pore networks in the

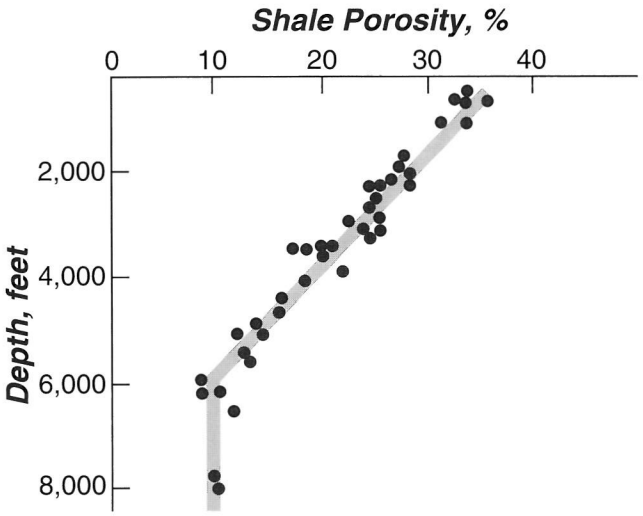

Figure 1. Shale porosity vs. depth for Venezuelan shales illustrating porosity decrease along two discrete straight-line segments. Hedberg (1936) drew a linear porosity line from 35 to 10% porosity. This was the only linear trend shown by Rieke and Chilingarian in their 1974 compilation of published porosity curves.

sandstones were composed predominantly of secondary porosity.

Several published examples of high secondary porosity in sandstones at depths >3 km emphasize that erroneous compaction models (such as assuming undercompaction) can result unless there is clear petrographic evidence that the porosity is primary (Meloche, 1985; Franks and Forester, 1984; Jansa and Noguera Urrea, 1990). Secondary porosity in sandstones is caused mainly by chemical diagenesis, not compaction. Consequently, shale porosities are more useful than sandstone porosities for following regional compaction trends and for recognizing the difference between normally compacted and undercompacted rocks–as will be discussed later. Note that, all porosity data in this report represents only shales, or in a few cases, limestones.

METHODOLOGY

All porosity measurements reported in this paper were carried out by Amoco using the method of Hinch (personal communication. See also, Hinch, 1980). Although shales in several thousand wells were analyzed, few of the data were published (Powley, 1993). Recently, part of Amoco's data bank was released through a cooperative project with the Gas Research Institute. The raw data from about 30 wells were used for the current paper.

Hinch's technique involves measuring the quantity of an organic liquid, Varsol, taken up by a dried, evacuated shale sample. Porosities measured by this procedure were compared with those obtained by Core Lab-

oratories on the same samples using a helium uptake method. The two methods agreed to within ±1.5% of each other. Helium tends to go into smaller pores than Varsol but, the Varsol is adsorbed more strongly on the mineral surfaces thereby forcing open some pores that may not be easily reached by helium. Although the two techniques were comparable, they both were between 5 and 10% lower than the porosity obtained on water saturated conventional cores. The reason for this apparent discrepancy is that a small amount of non-effective porosity (5 to 10% of the total porosity) develops when a sample shrinks on drying. The shrinkage tends to decrease with deeper samples with lower porosity. It is <5% of the porosity at depths >3 km. The interior sections of conventional connate water saturated shale cores give the most accurate porosities but they are too costly to take continuously.

A critical factor in making valid shale porosity measurements is that wet shale samples, including conventional cores containing large amounts of smectite and illite, must be analyzed very soon after collection. If not, they expand by hydration, resulting in porosities much higher than the original in situ values. Hydration also occurs in the sidewalls of a borehole during drilling. Consequently, if sidewall cores are taken at the end of a drilling operation they should not be used for porosity measurements. In this work, all cuttings were washed and dried as they arrived at the surface in order to prevent adsorption of enough water to cause hydration. Replicate experiments gave results within ±0.5% of each other.

Hinch (personal communication) also compared his porosity measurements with those obtained by various logging techniques (Figure 2). The dried cuttings (DC) line represents a moving average of porosity data determined on cuttings by the Hinch method. Porosities were averaged over a 250 ft (76 m) depth interval. The average was recalculated as each deeper sample was added with the shallowest being removed. Sixty-eight samples were analyzed from 4,000 ft (1,220 m) to 15,000 ft (4,575 m). The borehole gravity meter line (BGM) in the upper section of the well represents porosities calculated from wet bulk densities measured with this meter. Gravity is measured at two different depths in the well bore and the difference in gravity is proportional to the density of the rock. The advantage of this instrument is that the densities can be measured laterally in the rock formations through a circle 1,000 ft (300 m) in diameter. This avoids hydration effects around the borehole. Consequently, porosities obtained with this meter are close to the in situ porosities (Hinch, personal communication).

The curve in the lower section of the well in Figure 2 marked "Resistivity + % Illite (R+%I)" represents in situ porosity determined from the short normal resistivity and the percent of expandable mixed layer illite. According to Hinch (personal communication), E.R. Michaelis of Amoco found that the porosity of shales could be estimated from the following equation:

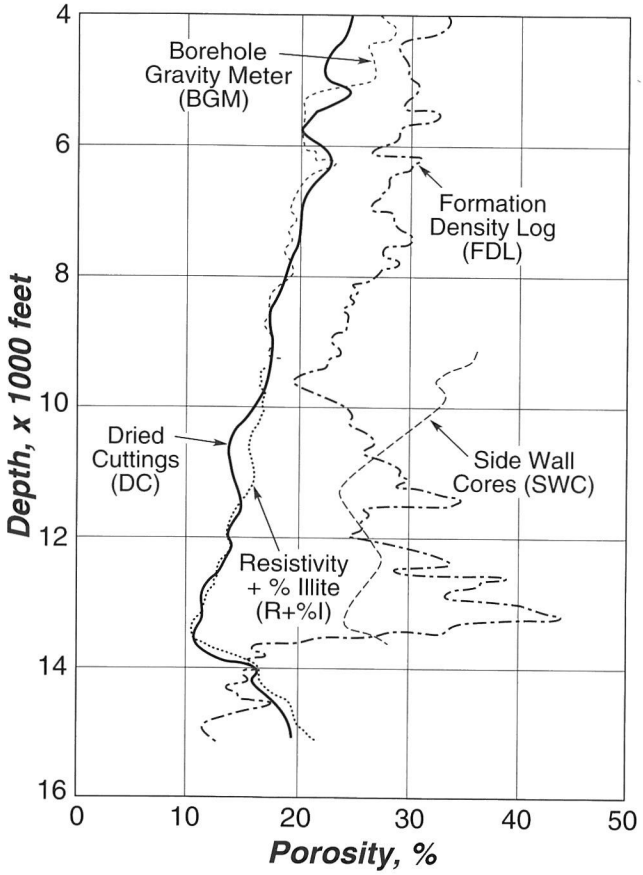

Figure 2. Laboratory porosity measurements on dried cuttings and sidewall cores compared to downhole porosity measurements made with the borehole gravity meter, formation density log, and to the in situ porosity calculated from the short normal resistivity and percent expandable mixed layer illite. This is Miami Corp. well no. 27 drilled by Amoco in Cameron Parish, Louisiana (Hinch, personal communication).

$$\text{Shale Porosity} = 4.88\left(\frac{I_{EML}^{0.35}}{R_{SN}^{0.47}}\right) \qquad (1)$$

where I_{EML} = % expandable mixed-layer illite and R_{SN} = short normal resistivity

The method, which requires X-ray diffraction analysis to determine the percent of expandable mixed layer illite, gives the porosities within ±2.5% of the value measured on a conventional water saturated core sample from the same depth (Hinch, personal communication). The most inaccurate porosities were measured with the formation density log (FDL) and with sidewall cores (SWC) as shown in Figure 2. Hinch believes this is due to extensive hydration of the shales around the well bore.

Exclusive use of either the formation density logs or sidewall cores to measure porosities can lead to the erroneous conclusion that the shales are undercompacted. Shale hydration at the borehole can be mistak-

en for undercompaction in deltaic sediments. The discussion which follows relies on the Hinch porosity analysis of cores and dried cuttings, thus avoiding these problems.

COMPACTION PROFILES OF NORMALLY COMPACTED SHALES

The first publication of Amoco data showing linear compaction appeared as a profile of density and porosity vs. depth for shales in a West Delta well offshore Louisiana—see well 20 in Figure 13 for porosity curve only (Bradley,1976). The data showed a linear increase in dry bulk density and decrease in porosity down to about 12,000 ft (3,660 m) followed by essentially no change in density or porosity to total depth (16,400 ft, 5,000 m). Bradley also showed other linear compaction profiles which indicated that a complete range of densities can be associated with abnormal pressures. He concluded that overburden stress is not the sole cause of abnormally high pressures because of this lack of any correspondence between overpressures and shale density.

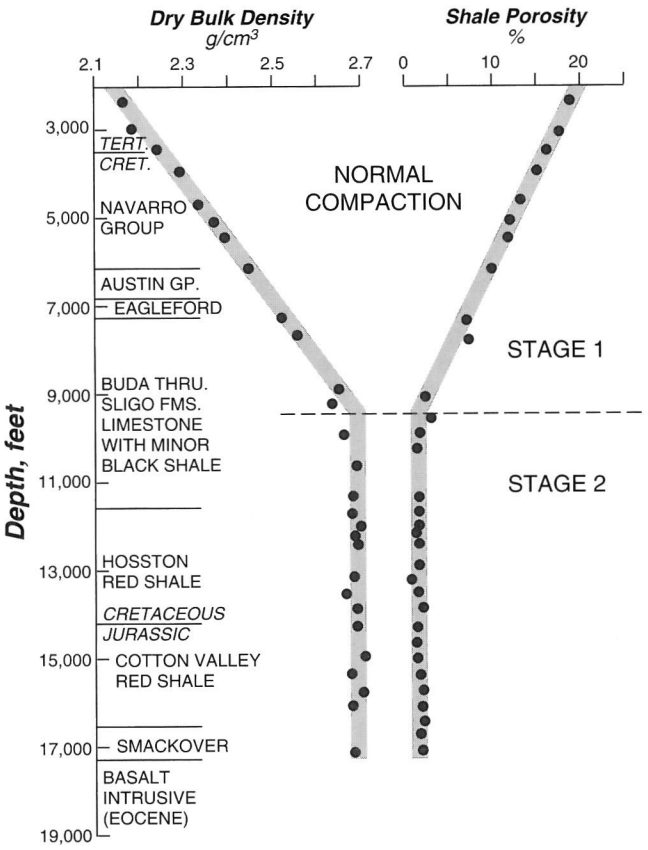

Figure 3. Shale dry bulk density and porosity vs. depth shown as two linear segments in angular end-to-end contact for the normally pressured Amoco Lena Buerger well in Frio County, Texas (Powley, 1993). These segments, divided by the dashed line, are called compaction Stages 1 and 2 by Hinch (1980) and Powley (1993). Black dots are individual sample measurements.

Hinch (1980) and Powley (1993) define the linear porosity change from 35 to 10% as compaction Stage 1 and the constant porosity interval as Stage 2 in normally compacting sediments. These are equivalent to Hedberg's mechanical deformation and recrystallization stages, respectively, which represent the two-stage compaction model in this paper.

For example, Figure 3 contains density and porosity data (black dots) for a normally compacted well, the Amoco Lena Buerger, in Frio County, Texas. Starting at a depth of 2,000 ft. (610 m) in Figure 3, the density increases and porosity decreases along straight line segments until they reach relatively constant values of 3% porosity and 2.7 g/cm^3 density at a depth of about 9,500 ft (2,900 m). From here to a basalt intrusive at 17,500 ft (5,335 m) there is no systematic decrease in porosity, indicating no compaction. We define this two stage compaction model as the normal compaction curve for this well. The low porosity of 3% in Stage 2 is due to the rocks containing mainly carbonates and red shales with kaolinite, both of which have very low mineral surface areas compared to smectite and illite.

Some geologists have speculated that the Stage 2 density and porosity lines in Figure 3 are caused by undercompaction. However, undercompacted shales are universally within overpressured compartments and there is no evidence that this well was ever overpressured (Powley, 1993). Overpressures can be recognized by drill stem tests, mud weights and resistivity logs. The Lena Buerger well was drilled with 9 lb/gal. mud to total depth. There was persistent lost circulation in the well and no shift from normal to low resistivities. All these observations indicated normal hydrostatic pressure throughout the well. The change from Stage 1 to 2 is not due to a change in lithology. The entire section through this shift is in Upper Cretaceous rocks with relatively similar lithologies.

This two-stage model can only be recognized by direct porosity and density measurements on samples from single wells. Composites of data from several wells generally show only a scatter of points.

Figure 4 is a map of the wells used in our study. The Lena Buerger well is no. 21, southwest of San Antonio. Table 1 contains the county or parish, state, latitude, longitude, operator, lease, and API well number for the wells cited. We included wells which covered the entire Gulf Coast area from the most southern part of Texas to the most eastern part of Louisiana. In order to limit the geological variables that would affect the porosity we only used wells from continuously sinking areas devoid of uplift and erosion or other structural changes that could cause variability in the porosity profile.

An important concept in this paper concerns the change from a continuous linear decrease in porosity with depth to no apparent decrease (no slope). The depth of this change is shown as a break in the slope of

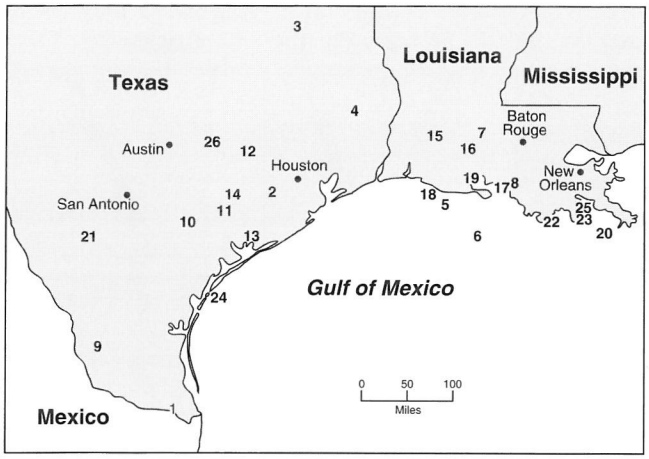

Figure 4. Location map for Gulf Coast wells in this study. Location data appears in Table 1.

the porosity lines in Figures 3, 5, 9, 11, 12, and 13. Four typical normal compaction porosity profiles from Louisiana and Texas (well numbers 5, 7, 8, and 11 in Table 1 and Figure 4) are shown in Figure 5. The vertical depth scales differ depending on the samples available for analysis. Each porosity profile is represented by two linear best fit segments. These correspond to compaction Stages 1 and 2, the second stage having no slope in the porosity vs depth profile. The break between Stages 1 and 2 occurs at a different depth in each of the four areas. This critical change can best be recognized from individual well data or closely spaced wells in the same oil field. If the data from the four wells in Figure 5 were composited the resulting curve would not be useful for determining the depth of the shift from a linear decrease to no decrease in porosity.

Our study confirms that of Bradley (1976) in showing no correlation between the top of Stage 2 and the onset of overpressures. The approximate tops of overpressures in these wells are: East Cameron, 13,000 ft (3,960 m), St. Landry, deeper than 15,000 ft (4,570 m), St. Mary, 15,500 ft (4,730 m), and Lavaca 10,000 ft (3,050 m). The interval from the top of Stage 2 to the top of the overpressure in these wells ranges between 1,000 and 5,000 ft (300 and 1,525 m).

The East Cameron well in Figure 5 shows a steady decrease in shale porosity until reaching a depth of about 7,800 ft (2,380 m). For the next 3,000 ft (915 m) or more of burial the shale porosity is remarkably uniform, showing no systematic increase or decrease. This contrasts with the Gulf Coast sandstones mentioned earlier by Loucks et al., (1984) which showed sandstone porosities ranging from 3 to 30% at these depths.

The St. Landry and St. Mary wells (7 and 8 in Table 1) show no systematic decrease in shale porosities starting around 12,000 ft (3,660 m) and 14,500 ft (4,420 m) respectively. The porosity of the St. Landry well is 12.1% at the top of Stage 2 and 12.3 % at the bottom of the hole, about 3,000 ft (915 m) deeper.

The well in Lavaca County, Texas (no. 11 in Table 1) is overpressured starting around 10,000 ft (3,050 m)

Table 1. Gulf Coast wells for which porosity profiles were studied. *Lease abbreviations: OCS = Outer Continental Shelf, OCSG = OCS Government land, SL = State Lease and, ST-TR = State Tract.

County	State	Latitude	Longitude	Operator	Lease*	API Number
1. Cameron Co.	TX	26.0S	97.7W	Pan American Co.	M.E. Wentz	(420610009700)
2. Fort Bend Co.	TX	29.7S	95.8W	Mobil Oil Corp.	B.C. Harwood	(421570297100)
3. Smith Co.	TX	32.3S	95.3W	Fairway O G Co.	Fairway et al.	(424230081800)
4. Tyler Co.	TX	30.9S	94.4W	Pan American Co.	Long Bel Co.	(424570005700)
5. E. Cameron Ph.	LA	29.5S	92.6W	Pan American Co.	SL 1186	(177030004800)
6. South Marsh Is.	LA	28.8S	92.0W	Pan American Co.	OCS 00785	(177070044800)
7. St. Landry Ph.	LA	29.7S	92.0W	Halbouty M.	K.S. Stelly et al.	(170972004100)
8. St Mary Ph.	LA	29.7S	91.3W	Pan Am	St. Mary B&T Co.	(171010199600)
9. Zapata Co.	TX	27.1S	99.0W	Union Prod	Jennings	(425050040600)
10. De Witt Co.	TX	29.1S	97.4W	Atlantic Richfield	Eliza Smith	(421230033200)
11. Lavaca Co.	TX	29.3S	96.7W	Magnolia	Simpson Heirs	(422850015500)
12. Washington Co.	TX	30.2S	96.4W	Shell	Jackson	(424770029142)
13. Matagorda Co.	TX	28.8S	96.3W	Tennessee Gas	B W Trull Estate	(423210230900)
14. Colorado Co.	TX	29.5S	96.6W	Shell Oil et al.	Plow Realty Co.	(420890049700)
15. Allen Ph.	LA	30.5S	92.8W	Pan American	J.A. Bell et al.	(170032000500)
16. Acadia Ph.	LA	30.3S	92.2W	Continental Oil	Faddy Arceneaux	(170010189600)
17. St. Mary Ph	LA	29.7S	91.5W	Humble Oil	A. Wettermark	(171010193200)
18. East Cameron OCS	LA	29.6S	93.0W	Pan American	OCS 1327	(177030023700)
19. Vermilion Ph.	LA	29.8S	92.0W	Pan American	Vermilion Land	(171132007900)
20. West Delta	LA	28.9S	89.6W	Pan American	OCSG 01088	(177190124600)
21. Frio Co.	TX	28.0S	99.0W	Pan American	Lena Buerger	(421630150900)
22. S. Timbalier	LA	29.1S	90.6W	Placid	SL 2857	(177150091400)
23. Grande Isle	LA	29.2S	90.0W	Humble Oil	SL 05013	(177170072600)
24. Mustang Island	TX	27.8S	96.8W	Atlantic	ST TR 726-L	(427020000900)
25. Plaquemines Ph.	LA	29.3S	89.6W	Amoco	Bastian Bay Fd.	(170750459300)
26. Lee Co.	TX	30.4S	96.9W	Pan Am	Willie Matejcek	(422870009100)

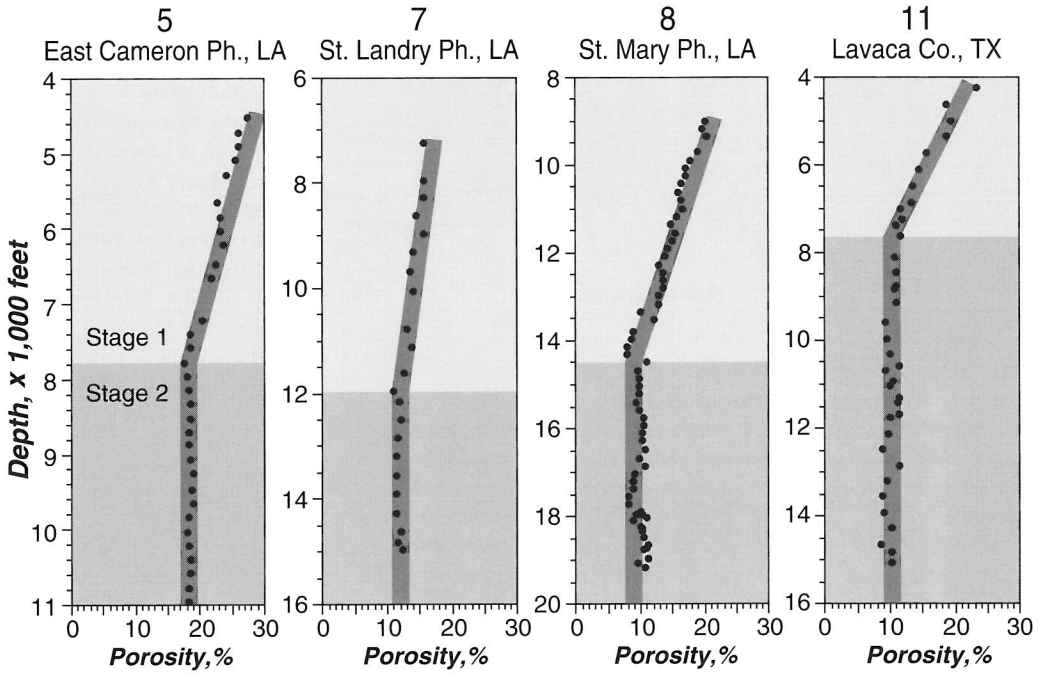

Figure 5. Porosity vs. depth for four wells in Louisiana and Texas (numbers 5, 7, 8 and 11 in Table 1). The vertical scales are different on these graphs due to limitations in the ranges of sampling.

where the pressure gradient is 0.69 psi/ft (16 kPa/m). Porosity data from two nearby wells in the same field were used to construct the curve (for this well) in Figure 5 because of gaps in the data from the individual wells. The linear decrease in porosity of Stage 1 extends to a depth of approximately 7,500 ft (2,290 m). At greater depths, there is no consistent decrease in porosity indicating no compaction through the next 7,500 ft (2,290 m) of burial. There is ~2,500 ft (760 m) of no compaction above the overpressured compartment.

Powley (1985, 1993) reported in his study of over 100 wells that the tops of deep overpressured compartments commonly occur a few thousand feet below the top of Stage 2. Less commonly they occur at the contact between Stages 1 and 2. Least common is when the overpressure top is found in compaction Stage 1. No clear relationship was reported by Powley between the top of Stage 2 and lithology. However, this top does seem to be related to subsurface temperatures. Hinch (1980) plotted the temperatures at the top of Stage 2 versus the age of the rocks for 65 wells in the Gulf Coast (Figure 6). Most of the temperatures were between 90° and 100°C (194° and 212°F) but they were as low as 82°C (180°F) in Cretaceous rocks and as high as 110°C (230°F) in Pleistocene rocks. This suggests that Stage 2 may be initiated by some process which depends on time-temperature conditions.

Statistical Analysis

Most basin models in recent years have assumed an exponential curve of porosity versus depth for their model based on the 1930 study of Athy (Dutta, 1987, Forbes et al., 1992, Ungerer et al., 1990, Waples and Okui, 1992). This assumption has prevailed despite evidence of linear porosity profiles as observed by Hedberg (1936) and discussed previously. Here we have examined the porosity data using statistical analysis. Our objective was to determine (1) whether an exponential or a linear variation in porosity with

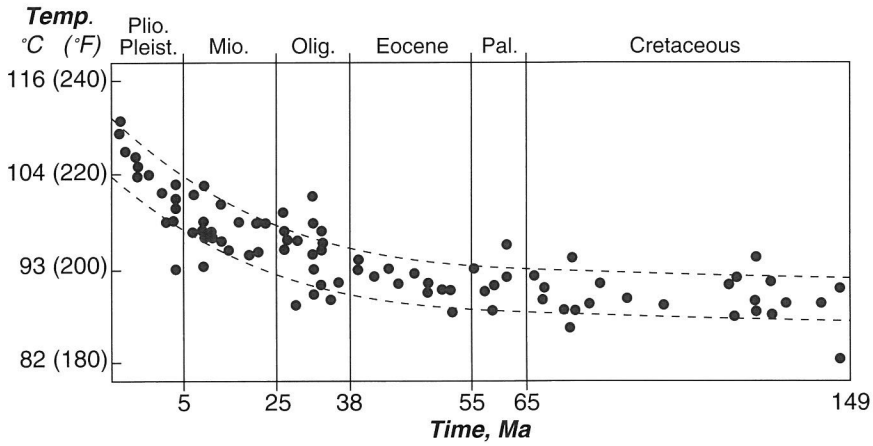

Figure 6. Relation between temperature and time (geologic epoch) of samples at the top of Stage 2 where porosity stops decreasing with depth (Hinch, 1980). The dashed lines enclose 80% of data as of 1980.

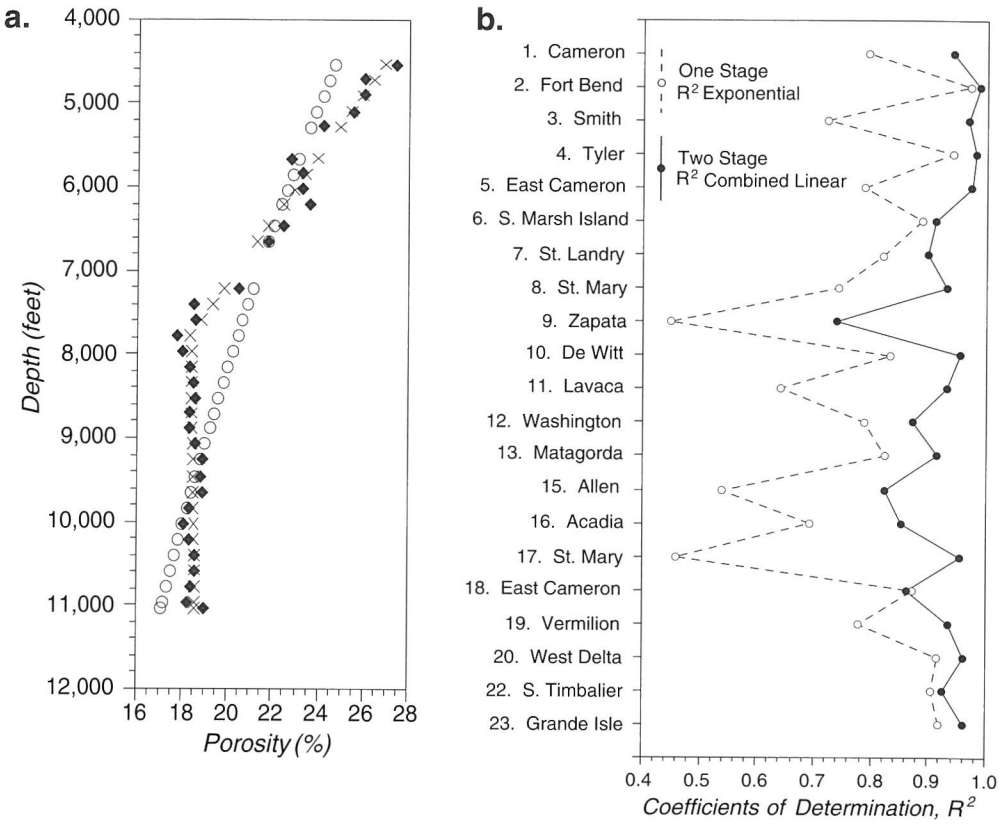

Figure 7. (a) Comparison of predicted porosities with measured porosity for an East Cameron Ph., La. well (no.5, Table 1). Symbols used: ◆ = measured porosity; O= predicted porosity from one-stage exponential curve fit (R^2 = 0.79); and × = predicted porosity from two-stage linear curve fit (R^2 = 0.95). (b) Graph showing the comparison of coefficients of determination (R^2) for a one-stage exponential curve fit and a two-stage linear curve fit for 21 normally compacted shale porosity-depth profiles in the U. S. Gulf Coast.

depth better fits the experimental data and (2) whether the compaction Stage 2 shows a constant porosity or a systematic increase or decrease with increasing depth.

If one considers porosity to decrease exponentially with depth over the entire data range, then correlation coefficients (r) should be indicative of this. However, porosity coefficients show a poor exponential relationship with increasing depth. In contrast, comparison of porosity changes modeled as two lines, either linear or exponential, yield much more convincing correlation parameters. Figure 7a shows an example of the predicted porosity (R^2) for a two-stage linear curve fit and a one-stage exponential curve fit compared to the actual measured porosity for the Louisiana, East Cameron well (no. 5 in Table 1). Clearly, the two-stage linear curve fits the measured porosities much better than the one-stage exponential curve. This also was true of all but one of the wells in this study as shown in Figure 7b (the exception is East Cameron, no. 18). For example, the R^2 exponential coefficient for the Lavaca well (no. 11) in Figure 7B is 0.642 compared to the two-stage linear coefficient of 0.933.

The more important aspect of our model, however, is to determine whether porosity in Stage 2 changes in a systematic way with increasing depth. To address this question, we used predicted porosity values from exponential and linear regression data solely for Stage 2. There is essentially no difference between coefficients of determination (R^2) for the two models in Stage 2 only. Both confirm that, within the errors of determination, there is no slope in the porosity versus depth curve for all wells except S. Marsh Island and Matagorda (no. 6 and 13) which show a slight decreasing and increasing porosity, respectively. We evaluated the upper and lower 95% confidence limits for the porosity versus depth slope determinations (Figure 8). These data confirm that porosity is constant throughout Stage 2 (i.e., there is no systematic change of porosity with increasing depth). The data support our concept that there is no compaction in Stage 2 for most normally compacted shales in the Gulf Coast.

Why Linear Compaction Profiles?

The conclusions in this paper apply to the Gulf Coast only. However, they also indicate that one cannot assume exponential porosity decreases in shales having porosities less than 30%. We believe that these deep linear profiles in the Gulf Coast may be related to mineralogy. It has been known since the 1960s that clay minerals compact exponentially while sandstones compact linearly (Chilingar and Knight, 1960; Atwater and Miller, 1965). Shales are composed largely of clay-sized particles which are assumed to be clay minerals, but what if they are quartz? Bradley (1993, personal communication) evaluated X-ray and elemental analyses of several hundred shales from the U.S. Gulf Coast. The shale sections in the cores were defined as shale by electric logs and visual inspection. The clay-size fraction (<4 μm) was found to consist of 74% quartz and

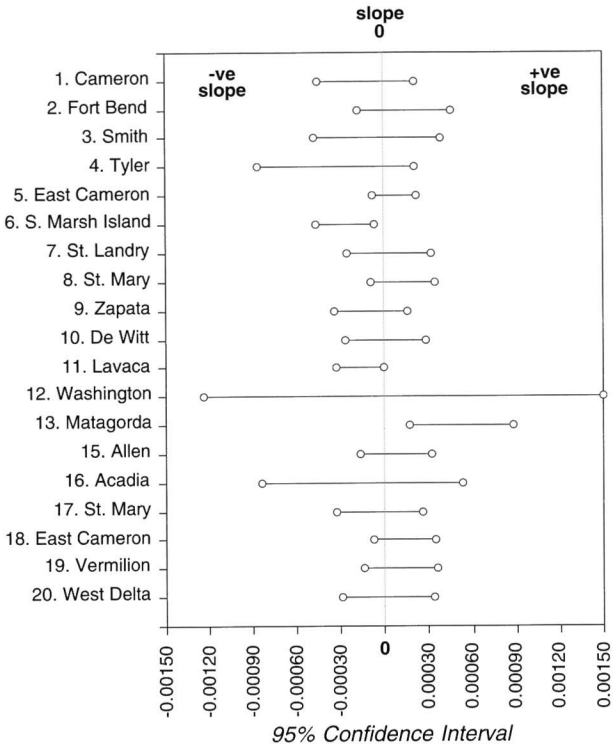

Figure 8. Graph showing Stage 2 porosity slope determinations for the wells in Figure 7b. Porosities of all but two of the wells (no. 6 and 13 in Table 1) have no slope within the 95% confidence interval. No. 6 has a slight negative slope (-ve) and well no. 13 a positive slope (+ve).

26% clay minerals. The average particle size of the quartz was 2 μm, and that of the clay minerals, 0.1 μm. The average Tertiary Gulf Coast shale based on Bradley's study contains 67% quartz, 7% feldspar, 20% clay minerals, 4% carbonate, and 1% organics and other minerals. Possibly this high content of clay-size quartz is causing the linear compaction profiles.

Why does the constant porosity Stage 2 reach a minimum value ranging from 3 to 18% with an average value around 10% (Figures 3, 5, 9, 11, 12, and 13)? This also appears to be related to mineralogy. For example, Figure 9 shows the porosity-depth profile for the Baltimore Canyon B-2 COST well drilled off the East Coast of the U.S.A. This is a normally pressured well with a normal compaction curve. Stage 2 porosities range from 3 to 6%. In Figure 10 the smectite-illite content of Stage 2 shales in this well are plotted against porosity and compared with similar data from a normally pressured Texas well. In this figure, a higher smectite-illite content equates with a higher minimum porosity. The Lena Buerger well in Figure 3, which has no smectite or illite, reaches a minimum porosity of 3% in Stage 2 while the typical Gulf Coast well with 20% smectite-illite averages 10% porosity in Stage 2.

In earlier work, Chilingar and Knight (1960) compacted clay minerals under 200,000 psi (13,800 MPa) pressure. The minimum porosity reached by smectite was 18% compared to 8% for kaolinite. Because of their enormous surface areas, smectite and illite retain far more water during burial than kaolinite, quartz and calcite. Powers (1967) showed that it takes 80,000 ft (24 km) of overburden pressure to remove the last two monomolecular layers of water from smectite. Thus shale porosities are unable to decrease much below 10% within current drilling depths when appreciable quantities of smectite and illite are present.

In constructing porosity and density profiles by depth, it is very important to plot the well data for shales only. Limestones and sandstones generally have different porosities than shales at the same depth. The differences with sandstones were mentioned in the introduction. Differences with limestones are shown in Table 2 for a well in Lee County, Texas (no. 26 in Table 1). Limestones are interbedded with shales at depths greater than about 12,000 ft (3,660 m) in this well. Porosities of the shales ranged between 10 and 16%. Limestones at the same depths have porosities of 2.6 to 7%. Indirect methods of estimating porosities, such as logging, would average these numbers.

COMPACTION PROFILES OF OVERPRESSURED SHALES

Figure 11 shows the two-stage normal compaction density and porosity profiles and a pressure-depth plot

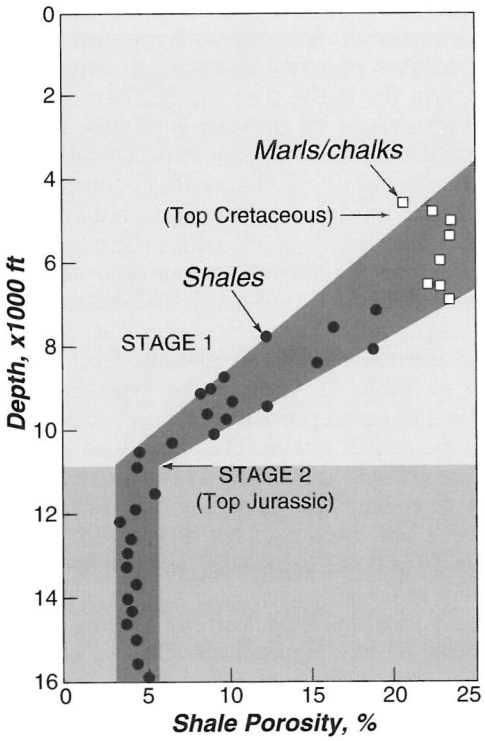

Figure 9. Shale porosity vs. depth for the normally pressured COST B-2 well in Baltimore Canyon, (offshore) New Jersey, U.S.A.

for a well in Bastian Bay Field, Plaquemines Parish, Louisiana (no. 25 in Figure 4 and Table 1). Here the shale reaches a minimum porosity of 10% at about 11,000 ft (3,350 m). The next 5,000 ft (1,525 m) or so represents the no compaction, constant porosity Stage 2 after which the porosity increases within an overpressured fluid compartment. An overpressure is defined as any pressure gradient above 12 kPa/m (0.53 psi/ft) which is the hydrostatic pressure of a saturated brine (Bradley and Powley, 1994). Drill stem tests within the top seal of Figure 11 show overpressures starting around 14,000 ft (4,270 m) within the Stage 2 interval. However, undercompaction, as indicated by an increasing porosity, is only evident below the second seal at about 16,000 ft (4,880 m). This is 2,000 ft (610 m) below the top of the overpressure.

A possible explanation for this is that the undercompaction originally extended to the top seal, but it has partially dewatered since forming. Powley (1993) defines an undercompacted shale as any shale which has not yet dewatered into the characteristic normal porosity-depth profile, in this case 10%. He claims that less than half of the deep (>3 km) overpressured rocks of the Gulf Coast are undercompacted. Examples of currently dewatering Gulf Coast shales are in Cameron Parish, Louisiana (Hinch, 1980) and Mustang Island (Hunt, 1996, p. 293). Additional examples are in Powley (1993).

Overpressures in the Gulf Coast may or may not lead to undercompaction. The Plaquemines Parish well in Figure 11 shows an increase in shale porosity (undercompaction) below 16,000 ft (4,880 m) but the well in Figure 12 in the Sheridan Field of Colorado County, Texas (no. 14 in Figure 4 and Table 1) shows no change in porosity or density with overpressure (Powley, 1993). There is a linear increase in dry bulk density and decrease in shale porosity down to a depth of about 8,700 ft. (2,650 m) at the top of Stage 2 (Figure 12). The top of an overpressured fluid compartment containing about 5,000 psi excess pressure occurs at around 12,000 ft (3,660 m) which is more than 3,000 ft (915 m) below the beginning of the constant porosity interval of Stage 2. There is no evidence of undercompaction occurring with the overpressures. Porosities and densities are essentially the same at 17,000 ft.

Table 2. Porosity of limestones and shales at similar depths in a Lee Co.,Texas well

Depth		Percent Porosity	
feet	*(meters)*	*Limestone*	*Shale*
12,940	(3,945)	2.6	10.6
13,850	(4,223)	3.7	12.6
14,900	(4,543)	5.8	15.8
15,260	(4,652)	7.0	14.8
15,620	(4,762)	6.2	13.5
15,950	(4,863)	5.5	13.2

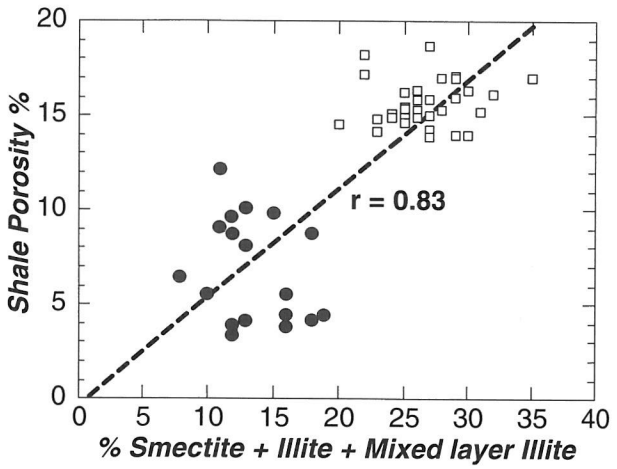

Figure 10. Correlation of shale porosity and smectite-illite content in normally pressured Stage 2 shales. Solid circles are shales from the Baltimore Canyon well (COST B-2), squares are shales from a Gulf Coast well offshore Texas.

(5,180 m) as at 8,700 ft (2,650 m). It is difficult to see how compaction can play any significant role in the development of these overpressures since there is no systematic reduction in porosity or increase in density starting above and extending through the overpressured fluid compartment.

The pressure measurements in Figure 12 (solid circles) are from drill stem tests. There is a suggestion of an increase in dry bulk density and corresponding decrease in porosity right at the seal in Figure 12 as might be expected.

Well numbers 15, 16, and 17 (Figure 4 and Table 1) in Allen, Acadia and St. Mary Parishes, Louisiana also show overpressures within the no compaction Stage 2 interval. For example, in the Allen well (no. 15) the pressure/depth gradient is 0.76 psi/ft (17.1 kPa/m), 1,500 ft (460 m) below the top of Stage 2.

HYDROCARBON GENERATION AS A CAUSE OF OVERPRESSURES

The top of the no compaction Stage 2 usually occurs between 90° and 100°C (194° and 212°F, Figure 6). Some geochemists believe these temperatures are not high enough to generate large quantities of hydrocarbons from Type III kerogen in rapidly depositing deltas. Time-temperature modeling based on the Arrhenius equation has indicated that although petroleum generation may start at temperatures as low as 60°C (140°F), the peak in oil and gas formation is usually at temperatures higher than 95°C (203°F) (Wood, 1988; Mackenzie and Quigley, 1988; Hunt and Hennet, 1992). Arrhenius kinetics for a Type III kerogen indicates a temperature of about 120°C (248°F) is required to initiate oil generation (Hunt, 1996, p. 159). Smith

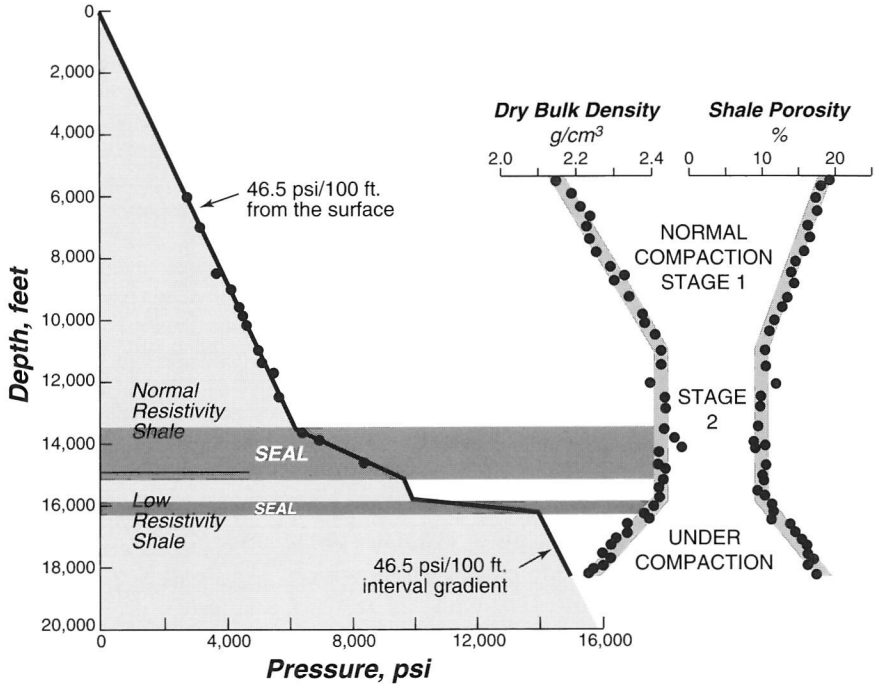

Figure 11. Porosity-density profiles of a well in Plaquemines Parish, Louisiana showing no compaction for 5,000 ft (1,525 m) above an overpressured sealed compartment and undercompaction within the compartment (Powley, 1993).

(1994) reported that <10% of the total gas yield from Type III kerogen is expelled at a vitrinite reflectance (R_o) of 1.3, whereas >60% is expelled at an R_o of 1.8, based on Shell Oil Company data files. These R_o values are roughly equivalent to paleotemperatures of 100° and 170°C, respectively. Because these temperatures are higher than those in Figure 6, it means that significant hydrocarbon generation occurs in the Gulf Coast below the top of compaction Stage 2. Overpressuring often peaks within this hydrocarbon generation window.

Figure 13 shows the porosity profile for an East Cameron well offshore Louisiana (no. 18, Figure 4) that is near a well that has been studied in considerable detail at the Woods Hole Oceanographic Institution. This area has continuously subsided and has not experienced uplift or erosion. The shales of well 18 are normally compacted with the break between compaction Stages 1 and 2 at about 10,700 ft (3,260 m).

The hydrocarbon generation window was determined by using pyrolysis techniques plus headspace analysis of canned cuttings such as were used in a South Padre, Texas well by Huc and Hunt (1980). The beginning of oil generation in the East Cameron well was at about 12,000 ft (3,660 m). The generation peak

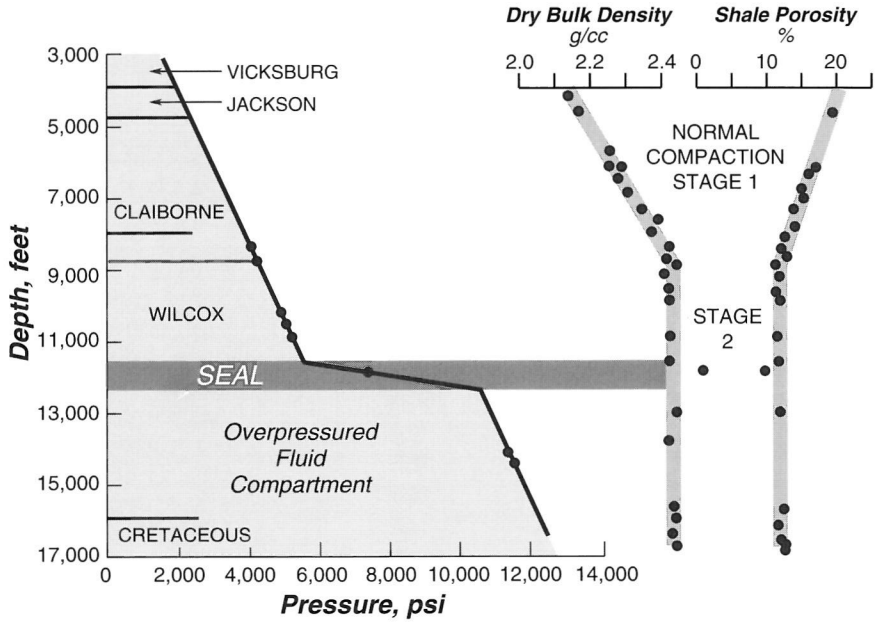

Figure 12. Compaction profile including dry bulk density and porosity for shales with depth for the Sheridan Field in Colorado County, Texas (no. 14 in Table 1). Pressure data points are by drill stem tests. Normal hydrostatic pressure extends from the surface to about 11,000 ft (3,350 m). The overpressure starts 3,000 ft (914 m) below the top of the constant porosity Stage 2. There is no evidence of undercompaction in this well and the porosity is relatively constant through the overpressured section (Powley, 1993).

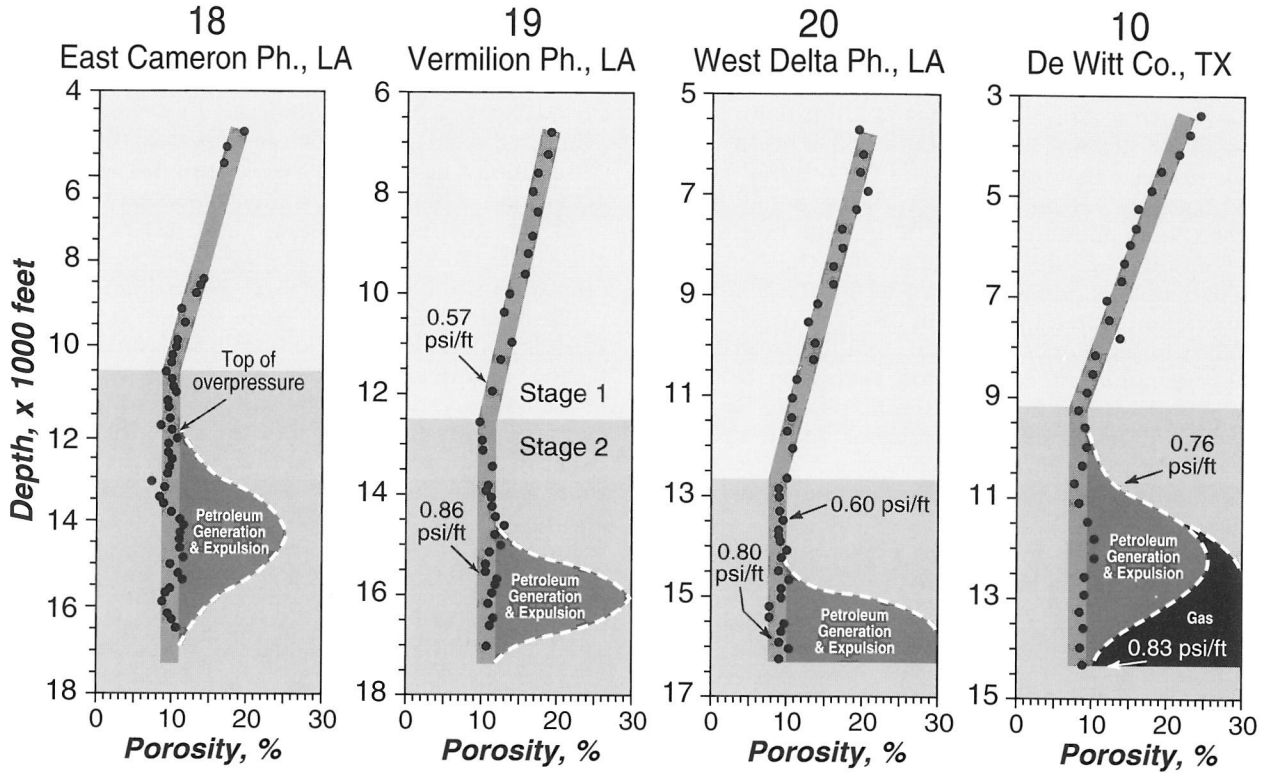

Figure 13. Porosity vs. depth for four Gulf Coast wells, showing the close relationship between the intervals of high overpressures and the petroleum generation and expulsion windows. All of these overpressures are in the intervals of no compaction. These wells are no. 10, 18, 19, and 20 in Table 1.

was in the 14,000 to 15,000 ft range (4,270–4,570 m). The distribution of individual hydrocarbons with depth indicated that considerable hydrocarbon expulsion and migration was occurring at 15,000 ft (4,570 m) (DOE Report no. COO-4392-4, 1981). Headspace analyses showed the C_2–C_8 hydrocarbons peaking at about 14,500 ft (4,420 m). Vitrinite reflectance values ranged from R_o = 0.65 to 0.9% through the hydrocarbon generation interval.

A. Yukler carried out a one-dimensional maturation model in this area for us using the model of Yukler and Kokesh (1984). Computed sterane isomerization ratios predicted that equilibrium should have been reached at about 15,000 ft (4,570 m). The computed hydrocarbon generation showed that the active oil generation zone is from 13,000 to 15,000 ft (3,960–4,570 m) with the peak at 15,000 ft corresponding to the equilibrium in the sterane isomerization ratios. The model also shows that the gas/condensate generation zone was from 15,000 ft (4,570 m) to the bottom of the well. The model results showed a good match with the Woods Hole experimental data.

Figure 13 shows the computed maturation interval in the East Cameron area (well no.18). There are about 4,000 ft (1,220 m) of rocks showing no compaction above the peak in oil expulsion and migration. The top of overpressure coincides with the start of petroleum generation at ~12,000 ft (3,660 m). Consequently, in this well, it appears that hydrocarbon generation is related to the generation of overpressures, but not to the cessation of compaction.

The second porosity profile in Figure 13 is for well no. 19 in the onshore Vermilion area of Louisiana. The top of the no compaction (Stage 2) is at about 12,500 ft (3,810 m) and the top of the overpressure is around 11,000 ft (3,350 m) This is an example of the overpressure starting in Stage 1. Data were available for constructing a burial history curve in this area for the Oligocene and Eocene formations. Using this curve for the base of the Oligocene Vicksburg group along with Arrhenius kinetics for Type III kerogen (Hunt, 1996, p. 159) it was possible to estimate the location of the oil window as shown in Figure 13. Generation was calculated as beginning around 15,000 ft (4,820 m) for the base of the Upper Oligocene with peak generation and expulsion extending about 1,000 ft (305 m) deeper. Although the porosity data for this well end at 17,000 ft (5,180 m) there is no significant decrease in porosity indicating no compaction. The high pressure/depth gradient of 0.86 psi/ft (19.4 kPa/m) is centered in the hydrocarbon generation window.

In 1974, La Plante developed a set of simultaneous equations designed for calculating the amounts of methane, carbon dioxide, water, and nitrogen as thermodynamically stable products generated during the conversion of kerogen to petroleum. He used this model to determine the depths at which petroleum and other volatiles were formed from the kerogen in three

wells in the Louisiana Gulf Coast. The porosity/depth plot for his well, in West Delta, Louisiana, is in Figure 13 (well no. 20). He found that the beginning of the oil window occurred around 14,000 ft (4,270 m) at a temperature of 205°F (96°C). At 16,500 ft (5,030 m) his calculations showed that about 10% of the original kerogen had been converted to hydrocarbons, mostly gas. This represented about one-third of the total hydrocarbon generating capability calculated for the kerogen using Arrhenius kinetics. Consequently, La Plante's (1974) model indicated that the oil plus gas window in this well extends deeper than the total depth drilled. There is no apparent compaction occurring in this interval based on the porosity/depth profile. Nevertheless, the pressure/depth gradient reaches 0.80 psi/ft (18 kPa/m) within the oil and gas generation window. No data was available for defining the top of the overpressure.

Yukler and Dow (1990) applied a quantitative basin analysis model to a drilling site within 6 miles (10 km) of the De Witt County Texas well in Figure 13 (well no. 10). They used data on wells in this area to determine the geologic evolution of the basin and to quantify pressure, temperature, organic matter maturation, and hydrocarbon generation histories. The hydrocarbon generation was determined from the kinetic equations given by Tissot and Espitalie (1975) with corrected cracking parameters and computed temperatures (Yukler, 1987). The top of the overpressure in this area is at about 10,000 ft (3,050 m).

Their model showed that the oil generation window for a mixed Type II, III kerogen began at a depth around 10,000 ft (3,050 m) and peaked at a depth around 11,808 ft (3,600 m). The oil generation phased out around 14,760 ft (4,500 m). However, active gas generation continued down to 18,040 ft (5,500 m). The increase in overpressure with depth in the De Witt well in Figure 13 correlates directly with the increase in gas generation computed by the Yukler and Dow model (1990). Thus, gas generation appears to be related to the overpressure. Compaction cannot be causing the overpressure since there is no decrease in porosity through the oil and gas generation window in any of these wells. All of these cases shown in Figure 13 support the concept that gas generation is causing the observed overpressures.

Several petroleum geologists have suggested that hydrocarbon maturation causes overpressuring and primary hydrocarbon migration. For example, Momper (1978) reported that primary hydrocarbon migration on a significant scale from a shale source rock occurs only after the kerogen has generated about 15 bbl of oil per acre-foot of rock (850 ppm). Momper's model calculated that at peak oil generation the conversion of organic matter to liquids and gases can cause a net volume increase of up to 25 percent over the original organic volume. In the restricted pore space of a fine-grained source rock, this would create a localized pressure build-up causing the opening of existing microfractures or formation of new ones with the expulsion of oil. Overpressures of 0.6 to 0.7 psi/ft (13.6 to 15.8 kPa/m) would be sufficient to reopen closed vertical fractures and possibly form new ones (Momper, 1981). After oil is expelled, the fractures close until the pressure builds up from subsequent generation. This results in the pulsed expulsion of oil until the generating system runs down. Generation *causes* migration. When generation stops, the primary migration stops (Hunt, 1996, p. 316–319).

Meissner (1978) came to a similar conclusion in studying the Bakken shale source rock of the Williston Basin. High overpressures (>0.6 psi/ft, >13.6 kPa/m) in the Bakken shale are confined both stratigraphically and regionally to that part of the shale that is actively generating oil. Pressures above and below the Bakken shale are slightly subnormal and pressures to the west and east in the immature, non-generating, shallower section of the Bakken are normal. Meissner concluded that active high-rate hydrocarbon generation was causing the high fluid formation pressures.

In the Altamont Field of the Uinta Basin of Utah, overpressures up to 0.8 psi/ft (18 kPa/m) are confined to the Upper Wasatch-Green River Black Shale, with normal pressures above and below (Hunt, 1979, p. 245). Based on comparisons of actual data to their models, both Sweeney et al. (1987) and Spencer (1987) concluded that hydrocarbon generation caused overpressures in the Altamont Field of the Uinta Basin.

Law (1984) studied source rocks and overpressures in the Upper Cretaceous and Lower Tertiary rocks of the Greater Green River Basin in Wyoming, Colorado and Utah. He found that abnormally high formation pressures in this basin are always associated with gas-bearing reservoirs, which suggests that the overpressures are caused by the generation of gas. A subsequent study by Law and Dickinson (1985) indicated that overpressured gas accumulations in the Rocky Mountain region are caused by the thermal generation of gas in low-permeability rocks where gas accumulation rates are higher than rates of gas loss.

Barker (1990) modeled the conversion of oil to gas at 12,000 ft (3,660 m) in an isolated system to determine if it could cause overpressures. He found that the conversion of less than 2% of oil to gas would create overpressures exceeding the fracture gradient. Although Barker's model applied to reservoirs, there is over 100 times as much disseminated oil in the source rocks of the world as in reservoirs (Hunt, 1972). Conversion of this residual oil to gas with deeper burial could create small fractures throughout the source rock comparable to those observed in the Green River Shale of the Altamont field, Uinta Basin, the Bakken Shale of the Antelope field, Williston Basin and the Bazhenov Shale of the Salym field, West Siberian Basin. All of these source rocks are highly overpressured and fractured within the oil generation zones almost exclusively. For example, Vernik (1994) reported that bedding-parallel microfractures are pervasive in the deepest part of the

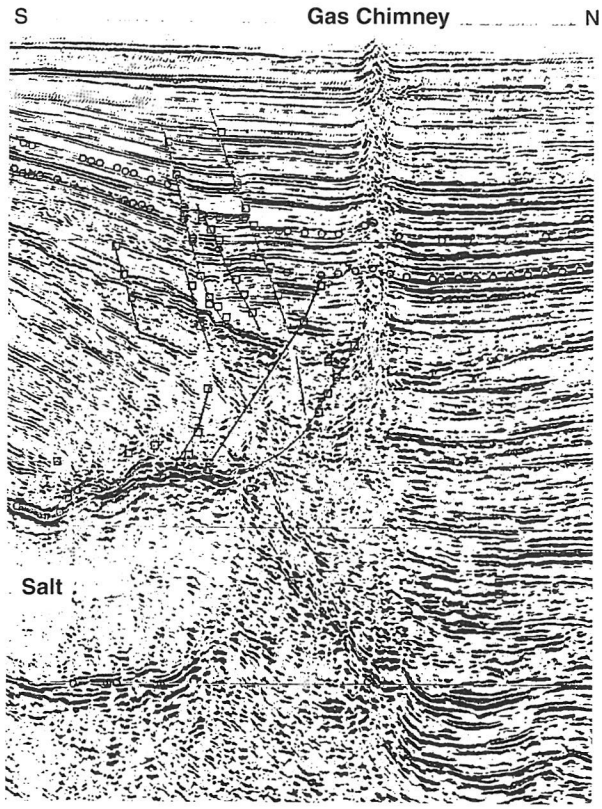

Figure 14. A 3-D seismic profile of a gas chimney rising from depths greater than 15,000 ft (4,570 m) up through Plio-Pleistocene sediments in the South Marsh Island area, offshore Louisiana. The gas plume is adjacent to a 7,000 ft (2,135 m) thick allochthonous Jurassic salt. The straight lines are faults, and boxes are crossline interpretations of horizons and faults (after Hunt, 1996, p.460).

Bakken Shale due to high overpressures caused by hydrocarbon generation. In the Deep Alberta Basin, there are isolated, overpressured carbonate gas reservoirs containing bitumen filled microfractures apparently resulting from the conversion of oil to gas (Marquez and Mountjoy, 1996).

Barker's model was primarily for methane generation but CO_2 is a major component of gases from both organic and inorganic sources in deltaic sediments such as in the Gulf Coast. In Miocene through Jurassic rocks of the Texas Gulf Coast the CO_2 ranges from <1 mole% in reservoirs at 7,000 ft (2,130 m) to 7 mole% in reservoirs at 12,000 ft (3,660 m) according to Franks and Forester (1984). The role of CO_2 in expelling hydrocarbons from shale source rocks is discussed further in our conceptual model of oil and gas expulsion.

Dahl and Yukler (1991) used a basin model to follow the geological and geochemical processes in the Oseberg area of the North Sea. Their computed pressure history showed that abnormal pressures occurred in the Viking group source rocks simultaneously with oil generation. A similar result was obtained in the Gulf Coast calculations discussed above that Yukler performed for us based on Yukler and Kokesh (1984). The computed excess pore pressures in these Gulf Coast calculations reached their highest level at a depth of 12,000 ft (3,660 m) and continued at that level to the bottom of the well.

Finally, Lewan (1987) found that oil and gas are expelled from chunks of source rocks in hydrous pyrolysis experiments where compaction plays no role.

Copious quantities of gas are migrating vertically from depths >3 km in the Gulf Coast. Figure 14 is an example of a three-dimensional seismic profile through Plio–Pleistocene sedimentary rocks in the South Marsh Island area offshore Louisiana. On the left is the edge of an estimated 7,000 ft (2,130 m) thick Jurassic salt contacting the Plio–Pleistocene sediments. On the edge of the salt is a gas chimney extending to the surface. Most gas chimneys in the Gulf Coast are small (about 400 m, 1,312 ft in diameter) and vertically oriented, so they are not usually seen on regional two-dimensional seismic grids. The gas plume in Figure 14 is not going up faults because it is nearly vertical, whereas the faults are at an angle. It is not syndepositional, slow acting, or continuous because there is no evidence of thinning of the sediment layers adjacent to the plume. It looks like a high-pressure gas blowout shooting up like a bullet. Some plumes look like wormholes in that they rotate slightly on the way up. The source of the gas in Figure 14 is difficult to determine. It may be gas spilling over from an accumulation under the salt or from a deeper overpressured compartment with a fractured seal (Hunt, 1996, p. 459).

A CONCEPTUAL MODEL OF COMPACTION AND HYDROCARBON GENERATION AND MIGRATION

The above discussion suggests the conceptual model illustrated in Figure 15. Grain dissolution compaction occurs in hydrostatically pressured shales from the base of mechanical compaction at ~500 m depth to the depth at which strata temperatures reach 85° to 110°C. Pressure dissolution at grain contacts is hypothesized to produce a plastic interpenetration of grain boundaries whose magnitude is a function only of the effective stresses pressing the grains together. Palciauskas and Domenico (1989) have shown that this kind of plastic penetration produces linear compaction. They derived a physical-chemical model for sand compaction from first principles. Remarkably, their model has no arbitrary parameters that need to be fitted. The predicted compaction depends only on the geometrical and physical properties of the load-bearing matrix grains. For a simple grain geometry and appropriate properties of quartz, their model predicts linear compaction of the right magnitude. Since Gulf Coast shales are 74% quartz in the clay-sized fraction (<4 μm) as previously stated, the model should be equally appropriate for describing shale compaction.

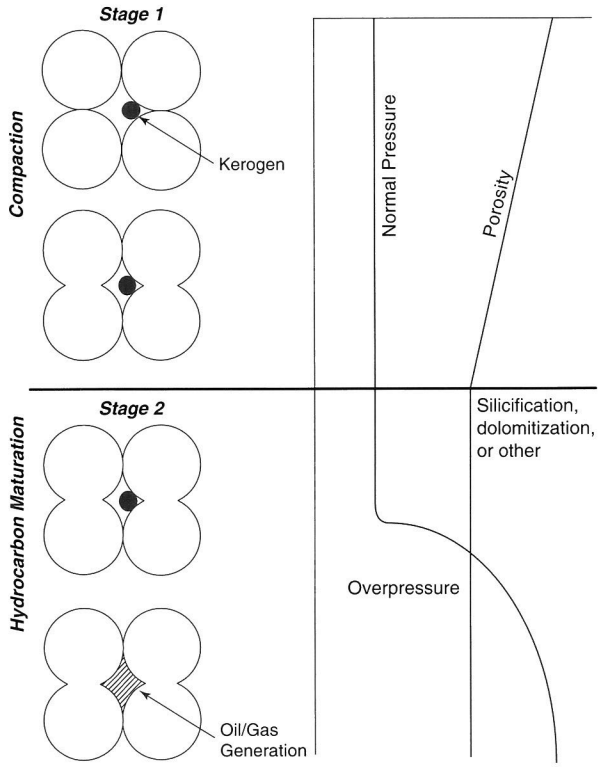

Figure 15. Conceptual model of compaction, overpressuring, and hydrocarbon generation. Linear compaction occurs until minimum adsorbed water and diagenetic reactions arrest further compaction. Overpressures are caused by the generation of hydrocarbon gases.

We suggest that compaction is arrested when only about three monomolecular layers of oriented water are still adsorbed on the mineral surfaces. Removal of the 3rd and 2nd layers from smectite-illite require 20,000 and 40,000 ft (6,100 and 12,200 m) of overburden, respectively (Powers, 1967). There also may be temperature dependent chemical changes involved such as silicification or dolomitization creating a rigid framework in the rock but we have no clear evidence for it.

Overpressures are generated in the organic-lean Gulf Coast rocks when maturation reactions occur whose products are of greater volume than the reactants. The positive volume change forces both the hydrocarbons and pore waters out of the source shales. If the shales have low enough permeability, overpressures are produced.

Figure 16 summarizes estimates of the densities and masses of the reactants and products of Type III kerogen maturation which is typical of the Gulf Coast. Consider the first stage of maturation, in which kerogen decomposes to bitumen, CO_2 and a residue, R. The change in volume of reactants and products depends mainly on the density of the CO_2 phase. Table 3 shows the density of CO_2, CH_4, and C_3H_8 along a hypothetical pressure-temperature depth profile. Temperatures increase at 25°C/km. Pressures increase hydrostatically to 2.9 km depth, then increase rapidly across a seal to lithostatic levels at 3.0 km depth, and thereafter again increase along a hydrostatic gradient. The density of CO_2 within the overpressured compartment on the high pressure side of the seal is ~0.89 g/cm^3. This density was calculated at 90°C and 660 bars using the Redlich Kwong equation of state. With this gas density, Figure 16 shows that the change in volume of the bitumen generation reaction depends on whether CO_2 dissolves or is isolated as a gas phase.

The volume changes shown in Figure 16 were calculated by dividing the mass of each reactant or product by its density and summing all reactants and products with the convention that reactant volumes are negative. The volume change was then converted to the change in volume within each cm^3 of sediment by multiplying by the grams of kerogen per cm^3 of sediment. The grams of kerogen per cm^3 sediment equals 3.6 x 10^{-2} for 1.5 wt% kerogen in the sediments. The kerogen is assumed to contain 67% carbon (TOC). The mass per unit volume was calculated from the relation TOC x ρ_g x $(1 - \phi)$, where TOC = 0.01, ϕ is the sediment porosity of 0.1 and ρ_g is the mineral grain density of 2.65 g/cm^3.

It is unlikely that any but the most organic-rich sediments will produce a separate CO_2 gas phase because CO_2 is very soluble in water. At 660 bars and 100°C, for example, a simple Henry's Law calculation indicates that water can dissolve ~0.4 grams of CO_2 per gram H_2O. Sediments with 1.0 wt% TOC contain 3.6 x 10^{-2} grams of kerogen per cm^3 sediment and can produce 7.2 x 10^{-3} g CO_2/cm^3. Pore waters can dissolve 4 x 10^{-2} g CO_2/cm^3 at 10% porosity. If the CO_2 dissolves, and we neglect the small volume change of the water caused by this dissolution, Figure 16 shows that the volume change of the bitumen generation reaction is negative (the products have less volume than the reactants). No overpressures will be generated, and no bitumen will be expelled from the source shales.

If on the other hand the CO_2 does not dissolve, the volume change of the reaction is positive. The products occupy more volume than the reactants, overpressures are produced, and CO_2 and bitumen are expelled from the shales. The overpressures may be very high and can be estimated following the approach of Barker (1990). The volume change of the bitumen-generating reaction, considering only the non-gas phases is 0.11 cm^3 per gram kerogen reacted. The reaction produces 4.5 x 10^{-3} moles of CO_2 per gram of kerogen reacted. The compressibility factor, z, for CO_2 at 660 bars and 90°C is 1.09. The gas law equation (below) relates pressure, P, in bars, volume, V, in cm^3, the moles of gas, n, temperature in degrees Kelvin (T_K = 373°K), and the gas constant, R = 83.14 cm^3 bar/mole °K:

$$P = \frac{83.14 z n T_K}{V} \qquad (2)$$

From this equation the pressure required to contain 4.5 x 10^{-3} moles of CO_2 in 0.11 cm^3 is 1,346 bars, or about twice lithostatic. If CO_2 does not dissolve, the

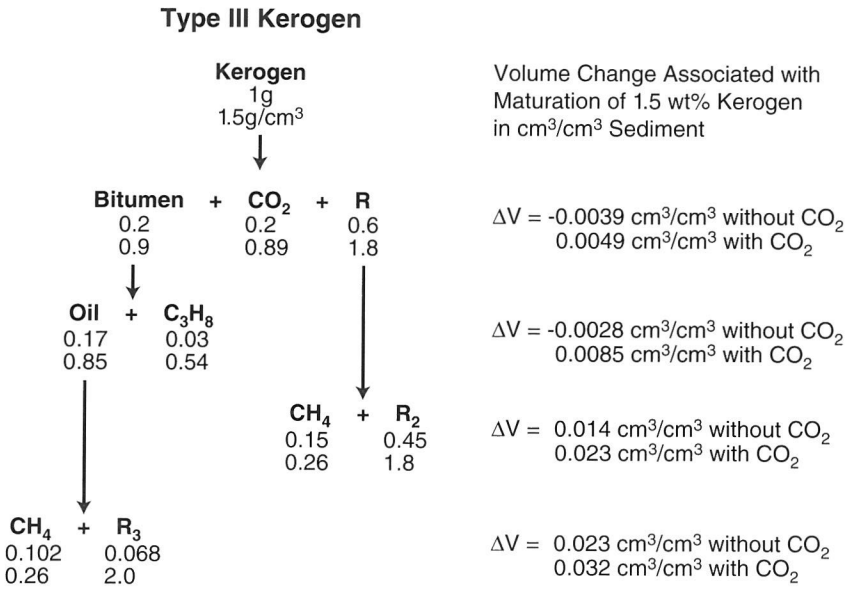

Figure 16. Maturation tree for Type III kerogen showing the grams of product (upper no.) generated from 1 gram of kerogen and the densities (lower no.) these products will have under overpressured conditions (90°C and 660 bars). Volume changes correspond to each of the four reactions shown. R_n = residue for that reaction.

overpressures will fracture the shale and expel CO_2 and bitumen (which is fluid at 90°C at these pressures).

If CO_2 dissolves, the first reaction that generates positive volume change is the methane generation reaction. Methane is much less soluble in water than is CO_2. At lithostatic pressures and realistic basin temperatures, the solubility of methane is about 5,000 ppm (Bonham, 1978). For sediments with porosities of 10%, about 5×10^{-4} g CH_4 can thus be dissolved per cm^3 sediment. For 1.5 wt% kerogen in the sediments this corresponds to 0.014 g CH_4 per gram of kerogen. Only about 10% of the methane generated by the third reaction in Figure 16 can be dissolved in the pore waters of 10% porosity sediment.

Assuming that all CO_2 and 10% of the CH_4 generated dissolves, the pressure produced by methane generation can be estimated by the same methods applied above. The non-gas volume (R_2 + R_3) created by the four reactions in Figure 16 is 0.41 cm^3/g kerogen reacted. The reactions generate 9.3 millimoles of methane, of which 0.93 millimoles are dissolved in the pore waters. With a z factor of 1.4 and 90°C temperatures, 845 bars are required to compress 8.4 millimoles of CH_4 into 0.41 cm^3. Pressures well in excess of lithostatic, which is about 660 bars at 3 km, can be generated by methane production.

The amount of hydrocarbon expulsion that can result from methane overpressures is indicated for Type III kerogen in Figure 16. The assumption is that a volume of pore fluids and hydrocarbons expelled equals the overall ΔV of reaction. The expelled volume can be expressed as a percentage of the original porosity if the figures in Figure 16 are divided by 0.1 and multiplied by 100. For 1.5 wt% kerogen in the sediments the first stage of methane generation could thus expel 14% of the bitumen, oil and pore fluids from a 10% porosity sediment.

Expulsion of both bitumen and oil would be greatly assisted by the presence of CO_2. At a subsurface temperature of 90°C (195°F) and pressure of 4,000 psi, about 500 standard cubic feet of CO_2 will dissolve in a barrel of 10° API oil reducing its viscosity by a factor of 30 (Murtada and Hofling, 1987).

Gas generation and the development of overpressures could of course arrest compaction by greatly reducing the effective stress on the mineral grains. This

Table 3. Densities (ρ) and compressibility (z) factors for CO_2, CH_4, and C_3H_8 along a hypothetical basin pressure-temperature profile. Parameters for CH_4 and C_3H_8 were computed from the Behar et al. (1985) equation of state. Parameters for CO_2 were computed from the Redlich Kwong equation of state. Z = depth.

Z (km)	T (°C)	P(bars)	ρ CO_2	z CO_2	ρ CH_4	z CH_4	ρ C_3H_8	z C_3H_8
1.4	50	140	0.60	0.38	0.10	0.88	0.50	0.46
2.4	75	240	0.66	0.56	0.14	0.94	0.49	0.75
2.6	80	260	0.67	0.59	0.15	0.95	0.49	0.81
2.9	87.5	290	0.68	0.63	0.16	0.98	0.49	0.88
3.0	90	660	0.89	1.09	0.26	1.36	0.54	1.8
3.4	100	700	0.89	1.13	0.26	1.39	0.53	1.9
3.8	110	740	0.89	1.17	0.26	1.43	0.54	2.0

mechanism for arresting compaction could be important in some cases, but for most of the Gulf Coast data summarized here, compaction is arrested above rather than at the top of the overpressure. Gas generation could affect permeability through capillary effects and could drive diagenetic reactions by changing pH. It is thus possible that gas generation and arrested compaction are indirectly related.

The most important aspect of this discussion is that gas generation provides an alternative to compaction as a mechanism for producing overpressures and expelling hydrocarbons. Where compaction is arrested, as in much of the deep Gulf Coast, gas generation becomes the most probable cause of overpressuring and hydrocarbon expulsion.

CONCLUSIONS

Direct measurements of porosity and density of shales reported by Bradley (1976), Hinch (1980), and Powley (1985, 1992, and 1993) laid the groundwork for showing that most shale compaction in the U.S. Gulf Coast occurs in two stages for porosities <30%. Powley's early work, reported by Hinch (1980), indicated that there is a time-temperature control of the abrupt change from a systematic decrease in porosity (compaction Stage 1) to no decrease (no compaction, Stage 2).

This paper supports those early conclusions by giving statistical evidence that a two-stage linear plot of shale porosity versus depth at porosities <30% fits the data better than a one-stage exponential plot. We show that in Stage 2 the porosity versus depth line has no slope indicating no compaction through as much as 10,000 ft (3,050 m) of rocks.

The peaks of oil, condensate and gas generation and expulsion and the tops of overpressures were commonly found to occur within intervals of no compaction, thereby, indicating that shale compaction cannot be the major contributor to overpressures or to the expulsion of hydrocarbons from these deep Gulf Coast rocks. The major cause of deep (>3 km) overpressures and the expulsion of hydrocarbons from these rocks appears to be the increase in volume of pore fluids caused by the thermal generation of gas.

The examples in this paper show that many porosity-depth relations in the Gulf Coast at porosities <30% can be described in two stages: (1) a linear decrease with depth, and (2) a deeper stage showing no decrease. This means that *the one stage exponential porosity-depth relation still used in most basin modeling today is not always valid.* Consequently, it is important to make direct shale porosity measurements on individual wells to define the type of porosity profile that actually exists before proceeding with a basin modeling program. The use of hypothetical curves not based on real data or the use of composites of data from several wells in a large area may lead to erroneous conclusions.

ACKNOWLEDGEMENTS *The authors particularly wish to thank the Amoco Production Co. for providing the basic porosity data and Henry H. Hinch, formerly of Amoco, for providing the information on his analytical methods, the smectite-illite data on shales, and for his constructive review of the manuscript. Thanks also are due to K.E. Peters, D.E. Powley, J.S. Bradley, and J.A. Curiale for critically reviewing various revisions of the manuscript. This work was supported by the Gas Research Institute, Contract No. 5091-260-2298. This is the Woods Hole Oceanographic Institution Contribution No. 8573.*

REFERENCES CITED

Athy, L.F., 1930, Compaction and oil migration: Bulletin of the American Association of Petroleum Geologists, v. 14, p. 25–36.

Atwater, G.I. and Miller, E.E. 1965, The effect of decrease in porosity with depth on future development of oil and gas reserves in south Louisiana: AAPG Bull., v 49, p. 334 abstract.

Barker, C.E., 1990, Calculated volume and pressure changes during the thermal cracking of oil to gas in reservoirs: AAPG Bull., v. 74, p. 1254–1261.

Behar, E., R. Simonet, and E. Rauzy, 1985, A new noncubic equation of state: Fluid Phase Equilibria, v. 21, p.237–255.

Bonham, L.C., 1978, Solubility of methane in water at elevated temperatures and pressures: AAPG Bull., v. 62, p. 2478–2481.

Bradley, J.S., 1976, Abnormal formation pressure: Reply: AAPG Bull., v. 60, p. 1127–1128.

Bradley, J.S. and D.E. Powley, 1994, Pressure compartments in sedimentary basins: A review. *in* P.J. Ortoleva (ed.), Basin Compartments and Seals: AAPG Memoir 61, Tulsa, American Association of Petroleum Geologists: p. 3–26.

Chilingar, G.V., and L. Knight, 1960, Relationship between pressure and moisture contents of kaolinite, illite, and montmorillonite clays: AAPG Bulletin, v. 44, p. 89–94.

Dahl, B., and A. Yukler, 1991, The role of petroleum geochemistry in basin modeling of the Oseberg area, North Sea. *in* R. K. Merrill (ed.), Source and migration processes and evaluation techniques, Treatise of petroleum geology handbook, Tulsa, The American Association of Petroleum Geologists. pp. 65–85.

Dickey, P.A., 1976, Abnormal formation pressure: discussion: AAPG Bull., v. 60, 1124–1128.

DOE Report No. COO-4392-4, 1981, Organic geochemistry of continental margin sediments.

Dutta, N.C., 1987, Fluid flow in low permeable porous media. *in* B Doligez (ed.), Migration of hydrocarbons in sedimentary basins. Collection 45, Paris: Editions Technip, pp. 567–596.

Forbes, P.L., P. Ungerer, and B.S. Mudford, 1992, A two-dimensional model of overpressure development

and gas accumulation in Venture Field, Eastern Canada: AAPG Bull., v. 76, p. 318

Franks, S.G., and R.W. Forester, 1984, Relationships among secondary porosity, pore-fluid chemistry and carbon dioxide, Texas Gulf coast *in* D.A. McDonald and R.C. Surdam (eds.) , Clastic diagenesis. AAPG Memoir 37. Tulsa: The American Association of Petroleum Geologists, pp. 63–80.

Hedberg, H.D., 1936, Gravitational compaction of clays and shales: Am. J. Sci., fifth series, 31, (184), 241–287.

Hinch, H.H., 1980, The nature of shales and the dynamics of hydrocarbon expulsion in the Gulf Coast Tertiary section in W.H. Roberts III and R.J. Cordell (eds.), Problems of Petroleum Migration: AAPG Studies in Geology, No. 10: Tulsa, The American Association of Petroleum Geologists, pp. 1–18.

Huc, A.Y. and J.M. Hunt, 1980, Generation and migration of hydrocarbons in offshore South Texas Gulf Coast sediments: Geochim. Cosmochim. Acta, v. 44, p. 1081–1089.

Hunt, J.M., 1972, Distribution of carbon in the crust of the earth: AAPG Bull., v. 56 , p. 2273–2277.

Hunt, J.M., 1979, Petroleum geochemistry and geology. first edition. San Francisco: W. H. Freeman and Company. 617 p.

Hunt, J.M. and R.J-C. Hennet, 1992, Modeling petroleum generation in sedimentary basins *in* J.W. Whelan and J.W. Farrington (eds.), Organic matter: productivity, accumulation and preservation in recent and ancient sediments: New York: Columbia University Press, pp. 24–52.

Hunt, J.M., 1996, Petroleum geochemistry and geology. second edition. New York: Freeman and Company. 743 pp.

Jansa, L.F., and V.H. Noguera Urrea, 1990, Geology and diagenetic history of overpressured sandstone reservoirs, Venture gas field, offshore Nova Scotia, Canada: AAPG Bull., v. 74, p. 1640–1658.

Korvin, G., 1984, Shale compaction and statistical physics: Geophysical Journal of the Royal Astronomical Society, v. 78, p. 35–50.

La Plante, R.E., 1974, Hydrocarbon generation in Gulf Coast Tertiary sediments: AAPG Bulletin, v. 58, p. 1281–1289.

Law, B.E., 1984, Relationships of source-rock, thermal maturity, and overpressuring to gas generation and occurrence in low-permeability Upper Cretaceous and Lower Tertiary rocks, greater Green River Basin, Wyoming, Colorado, and Utah *in* J. Woodward, F.F. Meissner, J.L Clayton (eds.), Hydrocarbon source rocks of the greater Rocky Mountain region. Denver: Rocky Mountain Association of Geologists. pp. 469–490.

Law, B. E. and W. W. Dickinson, 1985, Conceptual model for origin of abnormally pressured gas accumulations in low-permeability reservoirs: AAPG Bull., v. 69, pp. p. 1295–1304.

Lewan, M.D., 1987, Petrographic study of primary petroleum migration in the Woodford Shale and related rock units *in* B. Doligez (ed.), Migration of Hydrocarbons in Sedimentary Basins: Paris: Editions Technip, p.113–130.

Loucks, R.G., M.M. Dodge and W.E. Galloway, 1984, Regional controls on diagenesis and reservoir quality in Lower Tertiary sandstones along with Texas Gulf Coast *in* D.A. McDonald and R.C. Surdam (eds)., Clastic Diagenesis: AAPG Memoir 37. Tulsa Okla.: American Association of Petroleum Geologists, p. 15–45.

Mackenzie, A.S. and T.M. Quigley, 1988, Principles of geochemical prospect appraisal: AAPG Bull., v. 72, p. 399–415.

Marquez, X.M., and E.W. Mountjoy, 1996, Microfractures due to overpressures caused by thermal cracking in well-sealed Upper Devonian reservoirs, Deep Alberta Basin: AAPG Bull., v. 80, p. 570–588.

Meissner, F.F., 1978, Petroleum geology of the Bakken Formation, Williston Basin, North Dakota and Montana. Proceedings of 1978 Williston Basin symposium, "The Economic Geology of the Williston Basin," September 24–17, 1978, Montana Geological Society, Billings, pp. 207–227.

Meloche, J.D., 1985, Diagenetic evolution of overpressured sandstones - Scotian Shelf (abs.). 1985 Annual Convention Geological Association of Canada, Fredericton, N.B.

Momper, J.A., 1978, Oil migration limitations suggested by geological and geochemical considerations *in* Physical and chemical constraints on petroleum migration. Vol. 1. Notes for AAPG short course, April 9, 1978, AAPG National Meeting, Oklahoma City. 60 p.

Momper, J.A., 1981, The petroleum expulsion mechanism - a consequence of the generation process *in* AAPG Geochemistry for Geologists School. Notes for AAPG Short Course , Feb. 23–25, 1981, Denver Colorado

Murtada, H. and B. Hofling, 1987, Feasibility of heavy-oil recovery *in* R.F. Meyer (ed.), Exploration for Heavy Crude oil and Natural Bitumen, AAPG Studies in Geology No. 25, Tulsa, OK: American Association of Petroleum Geologists, pp. 629–643.

Palciauskas, V.V. and P. A. Domenico, 1989, Fluid pressures in deforming porous rocks: Water Res. Research, v. 25, p. 203–213.

Powley, D. E., 1985, Pressures, normal and abnormal. Lecture Notes, Techniques of Petroleum Exploration II. American Association of Petroleum Geologists School. South Padre Island, Sept 16–19, 1985.

Powley, D.E., 1992, Shale porosity-depth relations in normally compacted shale: Second Symposium on Deep Basin Compartments and Seals, Gas Research Institute Oklahoma State University, Sept. 29–Oct. 1, 1992. Stillwater, Oklahoma.

Powley, D.E., 1993, Shale compaction and its relationship to fluid seals. Section III, Quarterly report, Jan. 1993–Apr. 1993, Oklahoma State University to the Gas Research Institute, G.R.I., Contract 5092-2443.

Powers, M.C., 1967, Fluid-release mechanisms in compacting marine mud rocks and their importance in oil exploration: AAPG Bulletin, v. 51(7), p. 1240–1254.

Rieke III, H.H., and G.V. Chilingarian, 1974, Compaction of Argillaceous Sediments: New York, Elsevier Scientific Publishing Co., pp. 41–43.

Smith, J.T., 1994, Petroleum system logic as an exploration tool in a frontier setting *in* L.B. Magoon, and W.G. Dow (eds.) The petroleum system–from source to trap. AAPG Memoir 60. Tulsa: American Association of Petroleum Geologists. p. 31.

Spencer, C.S., 1987, Hydrocarbon generation as a mechanism for overpressuring in Rocky Mountain Region: AAPG Bull., v. 71, p. 368–388.

Storer, A., 1959, Constipamento dei sedimenti argillosi nel Bacino Padano, Giacimenti Gassiferi dell' Europa Occidentale. Rome: Acad. Nazionale dei Lincei, Rome. pp. 519–544.

Sweeney, J.J., A.K. Burnham, and R.L. Braun, 1987, A model of hydrocarbon generation from Type I kerogen: application to Uinta Basin, Utah: AAPG Bull., v. 71, p. 967–985.

Tissot, B., and J. Espitalie, 1975, L'évolution thermique de la metière organique des sédiments: application d'une simulation mathématique. Rev. Inst. Franc. Petrol., v. 30, p. 743–777.

Ungerer, P., J. Burrus, B. Doligez, P. Y. Chenet, and F. Bessis, 1990, Basin evaluation by integrated two-dimensional modeling of heat transfer, fluid flow, hydrocarbon generation, and migration: AAPG Bull., v. 74, p. 309–335.

Vernik, L., 1994, Hydrocarbon generation induced micro-cracking of source rocks: Geophysics, v. 59, p. 555–563.

Waples, D.W., and A. Okui, 1992, Overpressuring and hydrocarbon expulsion. (Abstract) American Association of Petroleum Geologists Annual Convention, Calgary, June 21–24. p. 137.

Wells, P.E., 1990, Porosities and seismic velocities of mudstones from Wairarapa oil wells of North Island, New Zealand, and their use in determining burial history: New Zealand Journal of Geology and Geophysics, v. 33, p. 29–39.

Wood, D.A., 1988, Relationships between thermal maturity indices calculated using Arrhenius equation and Lopatin Method: Implications for petroleum exploration: AAPG Bull., v. 72, p. 115–134.

Yukler, M.A., 1987, How essential is quantitative basin modeling in petroleum exploration? 7th Biannual Petroleum Congress of Turkey Proc., April 6–12.

Yukler, M.A., and W.G. Dow, 1990, Temperature, pressure and hydrocarbon generation histories in San Marcos Arch area De Witt County, Texas *in* D. Schumacher, and B.F. Perkins (eds.), Gulf Coast oils and gases: their characteristics, origin, distribution, and exploration and production significance: Proceedings of the Ninth Annual Research Conference, Society of Economic Paleontologists and Mineralogists Foundation, pp. 99–104.

Yukler, M.A., and F Kokesh, 1984, Review of models used in petroleum resource estimation and organic geochemistry *in* J. Brooks and D. Welte (eds.), Advances in Petroleum Geochemistry 1984, v. 1. London: Academic Press. pp 69–113.